

# Probing Primordial Stochastic Gravitational Wave Background with Multi-band Astrophysical Foreground Cleaning

Zhen Pan<sup>1,\*</sup> and Huan Yang<sup>1,2,†</sup>

<sup>1</sup>*Perimeter Institute for Theoretical Physics, Ontario, N2L 2Y5, Canada*

<sup>2</sup>*University of Guelph, Guelph, Ontario N2L 3G1, Canada*

(Dated: October 23, 2019)

The primordial stochastic gravitational wave background (SGWB) carries first-hand messages of early-universe physics, possibly including effects from inflation, preheating, cosmic strings, electroweak symmetry breaking, and etc. However, the astrophysical foreground from compact binaries may mask the SGWB, introducing difficulties in detecting the signal and measuring it accurately. In this Letter, we propose a foreground cleaning method taking advantage of gravitational wave observations in other frequency bands. We apply this method to probing the SGWB with space-borne gravitational wave detectors, such as the Laser Interferometer Space Antenna (LISA). We find that the spectral density of the LISA-band astrophysical foreground can be predicted with percent-level accuracy assuming 10-years' observations of third-generation GW detectors, e.g., Cosmic Explorer. After the foreground cleaning, LISA's sensitivity to the primordial SGWB will be substantially improved.

**Introduction.**— Primordial stochastic gravitational wave background (SGWB) has been conjectured to arise from various fundamental physical processes from the early universe [see e.g. Ref. 1, for a recent review], including the inflationary origin [2–7], cosmic strings [e.g., 8–12] and first-order phase transition due to electroweak symmetry breaking [e.g., 13–16]. Therefore measuring primordial SGWB at different frequencies will provide important information to understand our universe before recombination [17–22]. However, the total SGWB also contains contribution from astrophysical foreground of gravitational waves (GWs) from unresolved compact binaries [22], including galactic binary white dwarfs (BWDs), binary black holes (BBHs), binary neutron stars (BNSs) and possibly black hole-neutron star binaries (BHNSs). Removing the influence by the astrophysical foreground would be an essential step towards the measurements of primordial SGWB.

Inspired by recent discussions about the benefits of multi-band GW observations [23–30], we propose a multi-band foreground cleaning method and apply it to measuring the primordial SGWB in the LISA band [31]. The third-generation GW detectors, e.g. Cosmic Explorer (CE) [32] and Einstein Telescope (ET) [33], are expected to detect almost all BBH and BNS mergers in our universe [34]. With data from these ground-based detectors, we can reconstruct the underlying distribution of the BBH/BNS population and derive their contribution to the astrophysical foreground in the LISA band. In particular, we find that the astrophysical foreground can be predicted with percent-level accuracy with the CE running for 10 years. After removing this predicted astrophysical foreground from the LISA data, it can be shown that LISA's sensitivity to the primordial SGWB will be substantially enhanced.

In this work, we use BBHs as the proxy of astrophysical foreground sources, while the astrophysical foreground

sourced by BNSs and BHNSs can be cleaned in the same way. This multi-band foreground cleaning method does not apply for the galactic BWDs, because BWDs merge at a much lower frequency and never enter the band of ground-based detectors. Therefore we conservatively confine our analysis to a higher frequency band ( $f \gtrsim 5$  mHz) where the BWDs contribution to the foreground is negligible compared to that of BBHs.

We use the geometrical units  $G = c = 1$  and assume a flat  $\Lambda$ CDM cosmology with  $H_0 = 70$  km/s/Mpc,  $\Omega_\Lambda = 0.7$  and  $\Omega_m = 0.3$ .

## Stochastic GWs from Astrophysical Binaries.—

We now elaborate how to estimate the astrophysical foreground in the LISA band given a sample of mergers detected by the CE. Consider an observational period of LISA in  $[-T/2, T/2]$ , the average spectral density of the astrophysical foreground in this period is (see Appendix for a detailed derivation)

$$\hat{H}_A(f) = \frac{1}{T} \sum_i (|h_+(f)|^2 + |h_\times(f)|^2)_i \Theta_T^i(f) df, \quad (1)$$

where index  $i$  runs over all BBHs in our universe,  $\Theta_T^i(f) = 1$  if  $f \in [f_{t=-T/2}^i, f_{t=T/2}^i]$  and  $\Theta_T^i(f) = 0$  otherwise. Here  $f_t^i$  denotes the frequency of GW emitted at time  $t$  from  $i$ -th BBH, so that during the LISA observational period, only BBHs that cross the frequency  $f$  contribute to the summation in Eq. (1). In the quasi-circular approximation, one can show that the expectation value of  $\hat{H}_A(f)$  is

$$\langle \hat{H}_A(f) \rangle = \dot{N}_O \frac{f^{-7/3}}{6\pi^{4/3}} \int_0^\infty P(\zeta) \zeta^2 d\zeta, \quad (2)$$

where  $\langle \dots \rangle$  is the ensemble average over realizations of BBHs,  $\dot{N}_O$  is the merger rate seen in the observer's frame (i.e., number of mergers per unit time

detected by CE/ET),  $\zeta := (GM_z)^{5/6}/D_L$  and  $P(\zeta)$  is the corresponding distribution function normalized as  $\int_0^\infty P(\zeta)d\zeta = 1$ , with  $M_z = (1+z)M_c$  being the redshifted chirp mass, and  $D_L$  being the luminosity distance.

Physically Eqs. (1) and (2) display two different perspectives in understanding the astrophysical foreground. The former describes an event-based approach: the foreground consists of GWs from all unresolved (by the LISA) inspiral binaries, each of which will enter the ground detector band at a later time; therefore the foreground may be estimated by summing up contribution from events later identified by CE or ET. Eq. (2) states that the (ensemble average of) foreground can be obtained from the statistical distribution of the BBHs, which may also be measured precisely by ground-based detectors. Both approaches are equivalent (see the Appendix for derivation details). In the following sections, we will adopt the distribution-based approach and briefly discuss the application of Eq. (1) in an event-to-event subtraction in the Appendix.

To describe the underlying distribution of the BBH mergers, we need to specify the local merger rate density  $R(z)$  (number of mergers per comoving volume per unit of cosmic time) and the mass distribution  $p(m_1, m_2)$ . As a fiducial model, we assume  $R(z) = R_0 e^{-(z/10)^2}$  with  $R_0 = 65 \text{ Gpc}^{-3} \text{ yr}^{-1}$  [35], and

$$p(m_1, m_2) \propto \frac{1}{m_1(m_1 - m_{\min})}, \quad (3)$$

for  $m_{\min} \leq m_2 \leq m_1 \leq m_{\max}$ , with  $m_{\min} = 5M_\odot$  and  $m_{\max} = 42M_\odot$ . Combining the mass distribution  $p(m_1, m_2)$  with the merge rate density  $R(z)$ , it is straightforward to infer the merger rate  $\dot{N}_O$  in the observer's frame and the underlying distribution function  $P(\zeta)$  (see Fig. 1). Given  $R(z)$  and  $p(m_1, m_2)$ , we also generate many samples of BBH mergers. We then reconstruct the distribution function  $P(\zeta)$  assuming a number of merger events are recorded by ground-based detectors.

**Distribution Reconstruction.**— We model the Fourier-domain waveform  $h_A(f)$  of BBH mergers with the PhenomB waveform [36] which depends on 7 parameters: redshifted chirp mass  $M_z$ , redshifted total mass  $M_z$ , luminosity distance  $D_L$ , effective spin  $\chi$ , merger time  $t_0$ , merger phase  $\varphi_0$  and inclination angle  $\iota$ . The measured strain  $h(f)$  is related to  $h_A(f)$  by

$$h(f) = h_+(f)F^+(f; \theta, \phi, \psi) + h_\times(f)F^\times(f; \theta, \phi, \psi), \quad (4)$$

where  $F^{+\times}(f; \theta, \phi, \psi)$  are the detector response functions which depend on the sky location  $\theta, \phi$  and the polarization angle  $\psi$ . As an example, we consider a network with three detectors (assuming CE sensitivity) located in Australia, China and US respectively, with their locations and arm orientations specified in Table I, where the orientation is the angle between the bisector of two detector arms and the local west-to-east direction.

TABLE I. Location and orientation of the three ground-based detectors considered in this work.

	latitude	longitude	orientation
Detector 1	32° S	115° E	135°
Detector 2	38° N	104° E	90°
Detector 3	31° N	90° W	27°

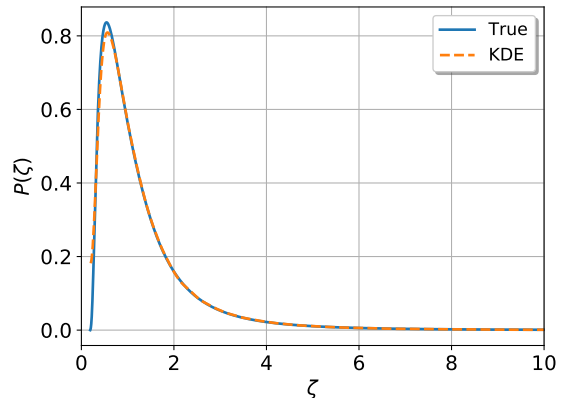


FIG. 1. The solid line is the underlying distribution of  $\zeta$  defined following Eq. (2), and the dashed line is the KDE reconstruction from  $4.5 \times 10^5$  merger events detected by the detector network, where  $\zeta$  is shown in units of  $M_\odot^{5/6} \text{ Gpc}^{-1}$ .

For each event, we estimate the parameter uncertainties using the Fisher matrix,

$$F_{\alpha\beta} = \sum_{d=1}^3 F_{\alpha\beta}^d = \sum_{d=1}^3 4 \int_0^\infty \frac{\Re[h_{d,\alpha}(f)h_{d,\beta}^*(f)]}{P_n(f)} df, \quad (5)$$

where  $h_d(f)$  is the strain in detector  $d$ ,  $h_{d,\alpha}$  is the derivative with respect to parameter  $\alpha$ , and  $P_n(f)$  is the noise spectral density of detectors [32]. The  $1\text{-}\sigma$  uncertainty of parameter  $\alpha$  is given by  $\sigma_\alpha = \sqrt{(F^{-1})_{\alpha\alpha}}$ . During an observational period  $T_D$ , we observe  $N_O$  mergers together with their best-estimated parameters  $\{\zeta_i\}$  ( $i = 1, \dots, N_O$ ), where  $\zeta_i$  is sampled from a Gaussian distribution with mean value  $\zeta_i^{\text{true}}$  and standard deviation  $\sqrt{\zeta_{i,\alpha}(F^{-1})_{\alpha\beta}\zeta_{i,\beta}}$ .

With a sample of  $\{\zeta_i\}$ , we can estimate the underlying distribution  $P(\zeta)$  using the kernel density estimator (KDE). We make use of the FFTKDE module from Python package KDEpy and determine the estimator bandwidth using Silverman's rule of thumb [37]. In Figure 1, we show the KDE reconstructed distribution function  $P(\zeta)$  from a sample of  $5 \times 10^5$  data points. The underlying distribution is reconstructed to a good precision except in the range of small  $\zeta$  [38].

To quantify the performance of the KDE reconstruction, we generate 100 realizations of  $N_O$  BBH mergers, “observe” each merger with the detector network and reconstruct  $P(\zeta)$  in each realization. With the recon-

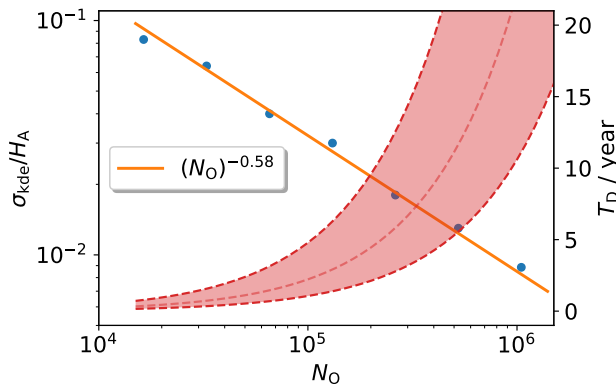


FIG. 2. The dots denote the fractional deviation of KDE reconstructed SGWB spectral density and the solid line is a power-law fit  $\sigma_{\text{kde}}/H_A \propto N_O^{-0.58}$ . The shadowed area denotes the uncertainty in the amount of mergers we expect the ground-based detectors to record in a given running time  $T_D$ , where the thin/dashed line in the center is the fiducial model we use in this work and the two thick/dashed lines correspond to merger rate density  $R_0 = 65^{+75}_{-34} \text{ Gpc}^{-3} \text{ yr}^{-1}$  [35].

structed  $P(\zeta)$ , we then calculate the spectral density  $H_{\text{kde}}(f)$  using Eq. (2). In Fig. 2, we show the fractional deviation  $\sigma_{\text{kde}}/H_A := \sqrt{\langle (H_{\text{kde}} - H_A)^2 \rangle} / H_A$  as a function of the total number of mergers  $N_O$ . We find that the fractional bias scales as  $\propto N_O^{-0.58}$ , being  $\sim 1.3\%$  for  $N_O = 4.5 \times 10^5$  which is roughly the number of BBH merger events in 10 years.

**Estimator of Primordial SGWB.**—For simplicity, let us consider two LISA detectors with output  $s_d(t) = h_d(t) + n_d(t)$  ( $d = 1, 2$ ), with  $h_d$  and  $n_d$  denoting the gravitational strain and the intrinsic noise in detector  $d$ , respectively. The case with a single detector is discussed in the Appendix. The SGWB signal can be measured by cross-correlating outputs from two detector because the detector noises  $n_1$  and  $n_2$  are not correlated, while the GW signals  $h_1$  and  $h_2$  are correlated. In the Fourier domain, the cross-correlation estimator is written as [39]

$$\hat{X} = \int_{-\infty}^{\infty} df \int_{-\infty}^{\infty} df' \delta_T(f - f') s_1^*(f) s_2(f') Q(f), \quad (6)$$

where  $\delta_T(f) := \sin(\pi f T) / (\pi f)$  is a finite-time approximation to the  $\delta$ -function,  $T$  is the running time of the two detectors and  $Q(f)$  is a filter function. The expectation value and variance of this estimator are [39]

$$\begin{aligned} \langle \hat{X} \rangle &= T \int_0^{\infty} H(f) \mathcal{R}_{12}(f) Q(f) df, \\ \sigma_X^2 &\approx \frac{T}{2} \int_0^{\infty} P_n^2(f) |Q(f)|^2 df, \end{aligned} \quad (7)$$

where

$$\mathcal{R}_{12}(f) = \int \frac{d\hat{\Omega}}{4\pi} e^{i2\pi f(\bar{x}_1 - \bar{x}_2) \cdot \hat{\Omega}} \sum_A F_1^{A*}(\hat{\Omega}, f) F_2^A(\hat{\Omega}, f),$$

is the overlap reduction function of the two detectors which we assume form a hexagonal pattern, and  $P_n(f)$  is the detector noise spectral density [20, 40–42]. In the ideal case of zero foreground, we can extract the primordial signal directly using the estimator (7). With the optimal filter  $Q(f) = H(f) \mathcal{R}_{12}^*(f) / P_n^2(f)$ , we obtain the maximized signal-to-noise ratio (SNR)

$$\text{SNR}_{\text{ideal}} = \sqrt{2T \int_0^{\infty} \frac{H^2(f)}{P_n^2(f)} |\mathcal{R}_{12}(f)|^2 df}. \quad (8)$$

In the presence of astrophysical foreground, we need to design an estimator of SGWB with foreground subtracted using the KDE reconstruction. In the LISA band, the foreground is dominated by the GW emission from BWDs at low frequencies and by that from BBHs at high frequencies (see upper panel of Fig. 3). The spectral density  $H_A(f)$  of the BBH foreground is known as a power law, while the spectral density of galactic BWD foreground depends on their orbital distributions. In the following discussion, we will confine our analysis to the frequency range  $f \geq f_{\text{min}} = 5$  mHz, where  $H_{\text{BWD}}(f)$  is negligible and  $H(f) \simeq H_P(f) + H_A(f)$  to a good approximation.

The spectral density of the astrophysical foreground  $H_A(f)$  can be estimated with  $H_{\text{kde}}$  elaborated in the previous section. From Eq. (7), we define an estimator of the spectral density of the primordial SGWB as

$$\hat{Y} = \hat{X} - T \int_0^{\infty} df H_{\text{kde}}(f) \mathcal{R}_{12}(f) Q(f), \quad (9)$$

with expectation value and variance

$$\begin{aligned} \langle \hat{Y} \rangle &= T \int_0^{\infty} df [H_P(f) + H_A(f) - H_{\text{kde}}(f)] \mathcal{R}_{12}(f) Q(f) \\ &:= Y_P + T \int_0^{\infty} df [H_A(f) - H_{\text{kde}}(f)] \mathcal{R}_{12}(f) Q(f), \\ \sigma_Y^2 &= \frac{T}{2} \int_0^{\infty} P_n^2(f) |Q(f)|^2 df. \end{aligned} \quad (10)$$

Therefore we have  $Y_P = \hat{Y} + \mathcal{N}(0, \sigma_Y) + \mathcal{N}(0, \sigma_A)$ , where  $\sigma_Y \propto \sqrt{T}$  is the statistical uncertainty due to detector noise and

$$\sigma_A = T \int_0^{\infty} \sigma_{\text{kde}} H_A(f) \mathcal{R}_{12}(f) Q(f) df$$

is the systematic bias due to the limited accuracy of the foreground measurement. Consequently, the SNR of estimator  $\hat{Y}$  scales as  $\sqrt{T}$  for small  $T$ , and saturates at  $Y_P/\sigma_A$  in the large  $T$  limit.

Without the multi-band measurement, the influence of astrophysical foreground may be removed by using its frequency dependence. For later convenience, we first define a binned estimator

$$\hat{X}_C := \int_{f \in C} df \int_{f' \in C} df' \delta_T(f - f') s_1^*(f) s_2(f') Q(f), \quad (11)$$

and also define an estimator  $\hat{Z}$ :

$$\hat{Z} = \hat{X}_{\pm[f_{\min}, f_*]} - \hat{X}_{\pm[f_*, f_{\max}]} , \quad (12)$$

where  $f_{\min} = 5$  mHz,  $f_{\max} = 1$  Hz, and  $f_*$  is determined by the constraint that the influence of astrophysical foreground is removed

$$\int_{f_{\min}}^{f_*} H_A(f) \mathcal{R}_{12}(f) Q(f) df = \int_{f_*}^{f_{\max}} H_A(f) \mathcal{R}_{12}(f) Q(f) df .$$

The mean value and the variance of  $\hat{Z}$  are

$$\begin{aligned} \langle \hat{Z} \rangle &= T \int_{f_{\min}}^{f_*} H_P(f) \mathcal{R}_{12}(f) Q(f) df \\ &\quad - T \int_{f_*}^{f_{\max}} H_P(f) \mathcal{R}_{12}(f) Q(f) df , \quad (13) \\ \sigma_Z^2 &= \frac{T}{2} \int_{f_{\min}}^{f_{\max}} P_n^2(f) |Q(f)|^2 df . \end{aligned}$$

In the upper panel Fig. 3, we present the spectral densities of LISA detector noise, stochastic GW foreground from various sources, the residual foreground ( $\sigma_{\text{kde}}/H_A = 1.3\%$ ), and two fiducial primordial SGWB signals with

$$\begin{aligned} H_{P,1}(f) &= 4.0 \times 10^{-43} (f/\text{Hz})^0 \text{ Hz}^{-1} , \\ H_{P,2}(f) &= 2.3 \times 10^{-48} (f/\text{Hz})^{-7/3} \text{ Hz}^{-1} . \end{aligned} \quad (14)$$

In the lower panel, we show the SNRs of estimators defined in Eqs. (9,12) for these two primordial signals. For comparison, we also show the SNR of the ideal estimator where there was no foreground contamination. Without foreground removal, the estimator  $\hat{Z}$  still can be used to detect the SGWB  $H_{P,1}$ , which has a different frequency dependence from that of the astrophysical foreground. However, for  $H_{P,2}$  which has the same frequency dependence as the astrophysical foreground, the SNR of  $\hat{Z}$  is zero. In contrast, with foreground cleaning, the estimator  $\hat{Y}$  can be used to measure the SGWB with any spectral density. We find that the foreground cleaning increases the LISA sensitivity by 25% – 55% for model  $H_{P,1}$ , and it enables the detection for model  $H_{P,2}$ .

**Discussion.**— For both estimators  $\hat{Y}$  and  $\hat{Z}$ , we have assumed an astrophysical foreground with a simple power-law spectral density  $H_A(f) \propto f^{-7/3}$ , which is true only if binaries have zero eccentricity. In the case of mildly eccentric binaries, the spectral density has a more complicated frequency dependence, which deviates from the simple power-law by  $\lesssim 50\%$  for BBHs with eccentricity  $e \lesssim 0.2$  [44, 45]. In addition, highly eccentric binaries formed through direct captures [46], as sources for ground-based detectors, are born above the LISA band. Therefore it is important to understand the eccentricity distribution of the BBHs for correctly determining the foreground spectral density in the LISA band.

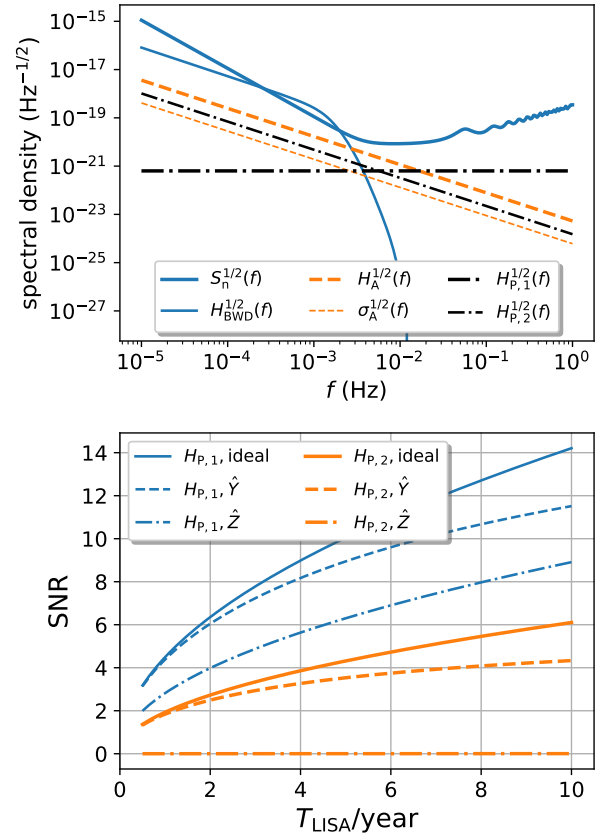


FIG. 3. Upper panel: the spectral densities of effective LISA detector noise  $S_n(f) = P_n(f)/\mathcal{R}(f)$ , unresolved binary white dwarfs  $H_{\text{BWD}}(f)$  [43], astrophysical foreground  $H_A(f)$  and residual foreground  $\sigma_A(f)$  after cleaning. Lower panel: green lines are SNRs of different estimator for primordial SWGB with spectral density  $H_{P,1}$  and orange lines are the corresponding SNRs for  $H_{P,2}$ .

Currently it is believed that there are two main formation channels: field binary evolution and dynamical formation in a dense stellar environment. While BBHs from the former channel are expected to have negligible eccentricities, dynamical formation has the potential to produce BBHs with high eccentricities. As implied by simulations done in Refs. [46, 47], a non-negligible fraction ( $\sim 28\% \times 20\% = 5.6\%$ ) of dynamically formed BBHs in dense globular clusters have large eccentricities ( $e_{0.01 \text{ Hz}} \gtrsim 0.1$  or  $e_{10 \text{ Hz}} \gtrsim 10^{-4}$ ) in the LISA band, and a even larger fraction ( $\sim 12\%$ ) of BBHs are born with larger eccentricities ( $e_{10 \text{ Hz}} \gtrsim 10^{-3}$ ) and never enter the LISA band. The latter ones can be readily measured by CE/ET which can distinguish mergers with eccentricities  $e_{10 \text{ Hz}} \geq 1.7 \times 10^{-4}$  [48], so that they will not affect the foreground estimation. As a result, we expect  $H_A(f)$  to have  $\sim 0.5 \times 5.6\% \times F_{\text{dy}}$  deviation from the circular approximation, where  $F_{\text{dy}}$  is the fraction of BBHs born in the dynamical channel. If dynamical formation is a

sub-dominant channel (say,  $F_{\text{dy}} < 0.4$ ), the deviation is likely at sub-percent level and can be safely ignored for our purpose. On the other hand, the loud BBH events detected by LISA may also provide us information about eccentricity distribution in the LISA band [45, 49–51].

*Acknowledgements.* This research was supported by the Natural Sciences and Engineering Research Council of Canada and in part by Perimeter Institute for Theoretical Physics. Research at Perimeter Institute is supported in part by the Government of Canada through the Department of Innovation, Science and Economic Development Canada and by the Province of Ontario through the Ministry of Economic Development, Job Creation and Trade.

---

\* [zpan@perimeterinstitute.ca](mailto:zpan@perimeterinstitute.ca)

† [hyang@perimeterinstitute.ca](mailto:hyang@perimeterinstitute.ca)

- [1] C. Caprini and D. G. Figueroa, *Classical and Quantum Gravity* **35**, 163001 (2018), [arXiv:1801.04268](https://arxiv.org/abs/1801.04268).
- [2] A. H. Guth, *Phys. Rev. D* **23**, 347 (1981).
- [3] A. D. Linde, *Physics Letters B* **108**, 389 (1982).
- [4] A. A. Starobinskiĭ, *Soviet Journal of Experimental and Theoretical Physics Letters* **30**, 682 (1979).
- [5] M. S. Turner, *Phys. Rev. D* **55**, R435 (1997).
- [6] R. Easther and E. A. Lim, *JCAP* **4**, 010 (2006), [astro-ph/0601617](https://arxiv.org/abs/hep-ph/0601617).
- [7] R. Easther, J. T. Giblin, and E. A. Lim, *Phys. Rev. Lett.* **99**, 221301 (2007).
- [8] T. W. B. Kibble, *Journal of Physics A Mathematical General* **9**, 1387 (1976).
- [9] A. Vilenkin and E. P. S. Shellard, *Cambridge Monographs on Mathematical Physics, Cambridge: Cambridge University Press, —c1994 ISBN 0521391539*. (1994).
- [10] R. Jeannerot, J. Rocher, and M. Sakellariadou, *Phys. Rev. D* **68**, 103514 (2003).
- [11] M. Sakellariadou, *Annalen der Physik* **15**, 264 (2006).
- [12] M. Sakellariadou, in *Lecture Notes in Physics, Berlin Springer Verlag*, Vol. 718, edited by W. G. Unruh and R. Schützhold (2007) p. 247, [hep-th/0602276](https://arxiv.org/abs/hep-th/0602276).
- [13] M. Kamionkowski, A. Kosowsky, and M. S. Turner, *Phys. Rev. D* **49**, 2837 (1994).
- [14] A. Kosowsky, M. S. Turner, and R. Watkins, *Phys. Rev. D* **45**, 4514 (1992).
- [15] C. Caprini, R. Durrer, and G. Servant, *Phys. Rev. D* **77**, 124015 (2008).
- [16] S. Iso, P. D. Serpico, and K. Shimada, *Phys. Rev. Lett.* **119**, 141301 (2017).
- [17] M. Kamionkowski, A. Kosowsky, and A. Stebbins, *Phys. Rev. Lett.* **78**, 2058 (1997).
- [18] U. Seljak and M. Zaldarriaga, *Phys. Rev. Lett.* **78**, 2054 (1997).
- [19] G. Hobbs, A. Archibald, Z. Arzoumanian, D. Backer, M. Bailes, N. D. R. Bhat, M. Burgay, S. Burke-Spolaor, D. Champion, I. Cognard, W. Coles, J. Cordes, P. Demorest, G. Desvignes, R. D. Ferdman, L. Finn, P. Freire, M. Gonzalez, J. Hessels, A. Hotan, G. Janssen, F. Jenet, A. Jessner, C. Jordan, V. Kaspi, M. Kramer, V. Kondratiev, J. Lazio, K. Lazaridis, K. J. Lee, Y. Levin, A. Lommen, D. Lorimer, R. Lynch, A. Lyne, R. Manchester, M. McLaughlin, D. Nice, S. Osłowski, M. Pilia, A. Possenti, M. Purver, S. Ransom, J. Reynolds, S. Sanidas, J. Sarkissian, A. Sesana, R. Shannon, X. Siemens, I. Stairs, B. Stappers, D. Stinebring, G. Theureau, R. van Haasteren, W. van Straten, J. P. W. Verbiest, D. R. B. Yardley, and X. P. You, *Classical and Quantum Gravity* **27**, 084013 (2010), [arXiv:0911.5206](https://arxiv.org/abs/0911.5206) [[astro-ph](https://arxiv.org/abs/astro-ph).SR].
- [20] P. L. Bender, A. Brillet, I. Ciufolini, A. M. Cruise, C. J. Cutler, K. Danzmann, F. Fidecaro, W. M. Folkner, J. H. Hough, P. A. Mcnamara, M. Peterseim, D. I. Robertson, M. R. e Rodrigues, A. Ruediger, M. Sandford, R. Schilling, B. Schutz, C. C. Speake, R. T. Stebbins, T. J. Sumner, P. Touboul, J.-Y. Vinet, S. Vitale, H. Ward, and W. Winkler, “LISA Pre-Phase A Report,” (1998).
- [21] S. Sato, S. Kawamura, M. Ando, T. Nakamura, K. Tsubono, A. Araya, I. Funaki, K. Ioka, N. Kanda, S. Moriawaki, M. Musha, K. Nakazawa, K. Numata, S.-i. Sakai, N. Seto, T. Takashima, T. Tanaka, K. Agatsuma, K.-s. Aoyanagi, K. Arai, H. Asada, Y. Aso, T. Chiba, T. Ebisuzaki, Y. Ejiri, M. Enoki, Y. Eriguchi, M.-K. Fujimoto, R. Fujita, M. Fukushima, T. Futamase, K. Ganzu, T. Harada, T. Hashimoto, K. Hayama, W. Hikida, Y. Himemoto, H. Hirabayashi, T. Hiramatsu, F.-L. Hong, H. Horisawa, M. Hosokawa, K. Ichiki, T. Ikegami, K. T. Inoue, K. Ishidoshiro, H. Ishihara, T. Ishikawa, H. Ishizaki, H. Ito, Y. Itoh, N. Kawashima, F. Kawazoe, N. Kishimoto, K. Kiuchi, S. Kobayashi, K. Kohri, H. Koizumi, Y. Kojima, M. Kokeyama, W. Kokuyama, K. Kotake, Y. Kozai, H. Kudoh, H. Kunimori, H. Kuninaka, K. Kuroda, K.-i. Maeda, H. Matsuhara, Y. Mino, O. Miyakawa, S. Miyoki, M. Y. Morimoto, T. Morioka, T. Morisawa, S. Mukohyama, S. Nagano, I. Naito, K. Nakamura, H. Nakano, K. Nakao, S. Nakasuka, Y. Nakayama, E. Nishida, K. Nishiyama, A. Nishizawa, Y. Niwa, T. Noumi, Y. Obuchi, M. Ohashi, N. Ohishi, M. Ohkawa, N. Okada, K. Onozato, K. Oohara, N. Sago, M. Saijo, M. Sakagami, S. Sakata, M. Sasaki, T. Sato, M. Shibata, H. Shinkai, K. Somiya, H. Sotani, N. Sugiyama, Y. Suwa, R. Suzuki, H. Tagoshi, F. Takahashi, K. Takahashi, K. Takahashi, R. Takahashi, R. Takahashi, T. Takahashi, H. Takahashi, T. Akiteru, T. Takano, K. Taniguchi, A. Taruya, H. Tashiro, Y. Torii, M. Toyoshima, S. Tsujikawa, Y. Tsunesada, A. Ueda, K.-i. Ueda, M. Utashima, Y. Wakabayashi, H. Yamakawa, K. Yamamoto, T. Yamazaki, J. Yokoyama, C.-M. Yoo, S. Yoshida, and T. Yoshino, in *Journal of Physics Conference Series*, Journal of Physics Conference Series, Vol. 840 (2017) p. 012010.
- [22] The LIGO/Virgo Scientific Collaboration, *Phys. Rev. Lett.* **118**, 121101 (2017).
- [23] A. Sesana, *Phys. Rev. Lett.* **116**, 231102 (2016).
- [24] E. Barausse, N. Yunes, and K. Chamberlain, *Physical Review Letters* **116**, 241104 (2016), [arXiv:1603.04075](https://arxiv.org/abs/1603.04075) [[gr-qc](https://arxiv.org/abs/gr-qc)].
- [25] S. Vitale, *Physical Review Letters* **117**, 051102 (2016), [arXiv:1605.01037](https://arxiv.org/abs/1605.01037) [[gr-qc](https://arxiv.org/abs/gr-qc)].
- [26] M. Tinto and J. C. N. de Araujo, *Phys. Rev. D* **94**, 081101 (2016), [arXiv:1608.04790](https://arxiv.org/abs/1608.04790) [[astro-ph](https://arxiv.org/abs/astro-ph).IM].
- [27] A. Sesana, in *Journal of Physics Conference Series*, Jour-

- nal of Physics Conference Series, Vol. 840 (2017) p. 012018, [arXiv:1702.04356 \[astro-ph.HE\]](#).
- [28] K. W. Wong, E. D. Kovetz, C. Cutler, and E. Berti, *Phys. Rev. Lett.* **121**, 251102 (2018).
- [29] S. Isoyama, H. Nakano, and T. Nakamura, *Progress of Theoretical and Experimental Physics* **2018**, 073E01 (2018), [arXiv:1802.06977 \[gr-qc\]](#).
- [30] Z. Carson and K. Yagi, *arXiv e-prints* (2019), [arXiv:1905.13155 \[gr-qc\]](#).
- [31] N. Bartolo, C. Caprini, V. Domcke, D. G. Figueroa, J. Garcia-Bellido, M. Chiara Guzzetti, M. Liguori, S. Matarrese, M. Peloso, A. Petiteau, A. Ricciardone, M. Sakellariadou, L. Sorbo, and G. Tasinato, *JCAP* **2016**, 026 (2016), [arXiv:1610.06481 \[astro-ph.CO\]](#).
- [32] B. P. Abbott, R. Abbott, T. D. Abbott, M. R. Abernathy, K. Ackley, C. Adams, P. Addesso, R. X. Adhikari, V. B. Adya, C. Affeldt, and et al., *Classical and Quantum Gravity* **34**, 044001 (2017), [arXiv:1607.08697 \[astro-ph.IM\]](#).
- [33] M. Punturo *et al.*, *Proceedings, 14th Workshop on Gravitational wave data analysis (GWDAW-14): Rome, Italy, January 26-29, 2010*, *Class. Quant. Grav.* **27**, 194002 (2010).
- [34] T. Regimbau, M. Evans, N. Christensen, E. Katsavounidis, B. Sathyaprakash, and S. Vitale, *Phys. Rev. Lett.* **118**, 151105 (2017).
- [35] The LIGO/Virgo Scientific Collaboration, (2018), [arXiv:1811.12940](#).
- [36] P. Ajith, M. Hannam, S. Husa, Y. Chen, B. Brügmann, N. Dorband, D. Müller, F. Ohme, D. Pollney, C. Reisswig, L. Santamaría, and J. Seiler, *Phys. Rev. Lett.* **106**, 241101 (2011).
- [37] <https://kdepy.readthedocs.io/en/latest/introduction.html#>.
- [38] The KDE estimator is smoothed over its bandwidth, therefore it does not capture variations with length scale much shorter than the bandwidth.
- [39] B. Allen and J. D. Romano, *Phys. Rev. D* **59**, 102001 (1999), [arXiv:9710117 \[gr-qc\]](#).
- [40] N. J. Cornish and S. L. Larson, *Class. Quantum Gravity* **18**, 3473 (2001).
- [41] N. J. Cornish, *Phys. Rev. D* **65**, 022004 (2001).
- [42] R. W. Hellings and W. A. Hiscock, *Phys. Rev. D - Part. Fields, Gravit. Cosmol.* **62**, 062001 (2000).
- [43] N. Cornish and T. Robson, in *Journal of Physics Conference Series*, Journal of Physics Conference Series, Vol. 840 (2017) p. 012024, [arXiv:1703.09858 \[astro-ph.IM\]](#).
- [44] E. A. Huerta, S. T. McWilliams, J. R. Gair, and S. R. Taylor, *Phys. Rev. D* **92**, 063010 (2015), [arXiv:0108028 \[arXiv:astro-ph\]](#).
- [45] L. Randall and Z.-Z. Xianyu, (2019), [arXiv:1907.02283](#).
- [46] C. L. Rodriguez, P. Amaro-Seoane, S. Chatterjee, K. Kremer, F. A. Rasio, J. Samsing, C. S. Ye, and M. Zevin, *Phys. Rev. D* **98**, 123005 (2018).
- [47] K. Kremer, C. L. Rodriguez, P. Amaro-Seoane, K. Breivik, S. Chatterjee, M. L. Katz, S. L. Larson, F. A. Rasio, J. Samsing, C. S. Ye, and M. Zevin, *Phys. Rev. D* **99**, 63003 (2019).
- [48] M. E. Lower, E. Thrane, P. D. Lasky, and R. Smith, *Phys. Rev. D* **98**, 083028 (2018).
- [49] K. Breivik, C. L. Rodriguez, S. L. Larson, V. Kalogera, and F. A. Rasio, *Astrophys. J.* **830**, L18 (2016).
- [50] A. Nishizawa, E. Berti, A. Klein, and A. Sesana, *Phys. Rev. D* **94**, 064020 (2016).
- [51] A. Nishizawa, A. Sesana, E. Berti, and A. Klein, *Mon. Not. R. Astron. Soc.* **465**, 4375 (2017), [arXiv:1606.09295](#).
- [52] E. S. Phinney, “A practical theorem on gravitational wave backgrounds,” (2001), [arXiv:astro-ph/0108028 \[astro-ph\]](#).
- [53] C. Cutler and É. E. Flanagan, *Phys. Rev. D* **49**, 2658 (1994).
- [54] J. D. Romano and N. J. Cornish, *Living Reviews in Relativity* **20** (2017), 10.1007/s41114-017-0004-1.
- [55] J. W. Armstrong, F. B. Estabrook, and M. Tinto, *Astrophys. J.* **527**, 814 (1999).
- [56] M. Tinto, J. W. Armstrong, and F. B. Estabrook, *Phys. Rev. D - Part. Fields, Gravit. Cosmol.* **63**, 021101 (2000).
- [57] C. J. Hogan and P. L. Bender, *Phys. Rev. D* **64**, 062002 (2001), [astro-ph/0104266](#).
- [58] T. Robson, N. Cornish, and C. Liug, *Class. Quantum Gravity* **36**, 105011 (2018), [arXiv:1803.01944](#).

## Stochastic GWs From Inspiral Binaries

Assuming the SGWB is isotropic, unpolarized and stationary, we can define its spectral density  $H(f)$  as (our definition is different from that of Ref. [39] by a factor  $8\pi$ ),

$$\langle h_A^*(f, \hat{\Omega}) h_B(f', \hat{\Omega}') \rangle = \frac{1}{2} \frac{\delta_{\hat{\Omega}, \hat{\Omega}'}}{4\pi} \delta_{AB} \delta(f - f') H(f), \quad (15)$$

with  $h_A(f, \hat{\Omega})$  being the waveform of gravitational waves coming from direction  $\hat{\Omega}$  with polarization state  $A \in \{+, \times\}$  written in the Fourier domain. The spectral density  $H(f)$  is related to the energy density of the SGWB by

$$\rho_{\text{GW}} = \frac{\pi}{2} \int_0^\infty f^2 H(f) df, \quad (16)$$

which in turn relates to the energy fraction of GWs in a logarithmic frequency bin  $\Omega_{\text{GW}}(f)$  by

$$\Omega_{\text{GW}}(f) := \frac{1}{\rho_{\text{crit}}} \frac{d\rho_{\text{GW}}}{d \ln f} = \frac{4\pi^2}{3H_0^2} |f|^3 H(|f|), \quad (17)$$

where  $\rho_{\text{crit}} := 3H_0^2/8\pi$  is critical energy density to close the universe.

The energy density of GWs averaged over all inspiral binaries in different directions  $\hat{\Omega}$  and a period of time  $[-T/2, T/2]$  is [52]

$$\begin{aligned} \hat{\rho}_{\text{GW}} &= \frac{1}{T} \sum_i \int_{-T/2}^{T/2} S_i(t) dt \\ &= \frac{1}{T} \sum_i \int_{-T/2}^{T/2} \frac{1}{16\pi} (\dot{h}_+^2 + \dot{h}_\times^2)_i dt \\ &= \frac{\pi}{2T} \sum_i \int_{f_-^i}^{f_+^i} f^2 (|h_+(f)|^2 + |h_\times(f)|^2)_i df, \end{aligned} \quad (18)$$

with index  $i$  running over all BBHs in the universe,  $S_i(t)$  being the energy flux of GWs emitted by the  $i$ -th BBH, dots denoting time derivative and  $f_\pm^i = f^j|_{t=\pm T/2}$  being the GW frequency of  $i$ -th BBH at  $t = \pm T/2$ . According to Eqs.(16) and (18), we find the spectral density of the astrophysical foreground averaged over time period  $[-T/2, T/2]$  is

$$\hat{H}_A(f) = \frac{1}{T} \sum_i (|h_+(f)|^2 + |h_\times(f)|^2)_i \Theta_T^i(f), \quad (19)$$

where  $\Theta_T^i(f) = 1$  if  $f \in [f_-^i, f_+^i]$  and  $\Theta_T^i(f) = 0$  otherwise.

To obtain the mean value of  $\hat{H}_A(f)$ , we first consider a sample of BBHs with same redshift  $z_s$ , same chirp mass  $M_s$  and merger rate  $\dot{N}_s$ . For this sample, all BBHs evolve along the same frequency-time curve  $f(t - t_{\text{merger}}^i)$ , i.e.,  $\frac{1}{T} \langle \sum_s \Theta_T^s(f) \rangle$  is independent of frequency  $f$  and is equal to  $\dot{N}_s$ . Therefore, we have

$$\langle \hat{H}_A(f) \rangle_s = \langle (|h_+(f)|^2 + |h_\times(f)|^2)_s \rangle \times \dot{N}_s. \quad (20)$$

Now consider BBHs in the real universe, with a merger rate density  $R(z)$  (number of mergers per comoving volume per unit of cosmic time local to the event) and the chirp mass distribution  $p(M_c)$ , we have the merger rate  $\dot{N}_s(z, M_c) dz dM_c = \frac{R(z)}{1+z} dV_c(z) p(M_c) dM_c$  and the mean value of  $\hat{H}_A(f)$  [52]

$$\langle \hat{H}_A(f) \rangle = \int_0^\infty \int_{M_{c,\min}}^{M_{c,\max}} \left\langle \sum_A |h_A(f)|_s^2 \right\rangle \dot{N}_s dz dM_c, \quad (21)$$

where  $dV_c(z) = 4\pi r^2(z)/H(z) dz$  is the comoving volume element, with  $r(z) = \int_0^z dz/H(z)$  being the comoving radial distance and  $H(z)$  being the Hubble expansion rate at redshift  $z$ . In the quasi-circular approximation, the waveform in the LISA band is [e.g., 53]

$$\begin{aligned} h_+(f) &= \frac{1 + \cos^2 \iota}{2} \sqrt{\frac{5}{24}} \frac{(GM_z)^{5/6} f^{-7/6}}{\pi^{2/3} D_L} e^{-i\Psi(f)}, \\ h_\times(f) &= i \cos \iota \sqrt{\frac{5}{24}} \frac{(GM_z)^{5/6} f^{-7/6}}{\pi^{2/3} D_L} e^{-i\Psi(f)}, \end{aligned} \quad (22)$$

where  $\iota$  is the inclination angle of the binary with respect to observers on the earth,  $\mathcal{M}_z = (1+z)M_c$  is the redshifted chirp mass,  $D_L$  is the luminosity distance and  $\Psi(f)$  is the wave phase. Plugging Eq. (22) into Eq. (21), we find

$$\langle \hat{H}_A(f) \rangle = \dot{N}_O \frac{f^{-7/3}}{6\pi^{4/3}} \int_0^\infty P(\zeta) \zeta^2 d\zeta, \quad (23)$$

where

$$\dot{N}_O = \int_0^\infty \int_{M_{c,\min}}^{M_{c,\max}} \dot{N}_s(z, M_c) dz dM_c,$$

is the merger rate seen in the observer's frame,  $\zeta = (GM_z)^{5/6}/D_L$  and  $P(\zeta)$  is the corresponding probability distribution.

## One detector, two channels

In the main text, we have outlined the foreground cleaning with KDE reconstruction assuming two LISA detectors for convenience, where the stochastic GWs can be separated from detector noise by cross-correlating the two detector outputs. For the proposed LISA mission, there will be a single detector and we may detect the SGWB by utilizing the ‘‘null’’ channel which is blind to GW signals for detector noise calibration, in combination with the normal Michelson (m) channel [54]. In reality, a good approximation to the ideal null channel is the symmetrized Sagnac (ss) channel whose response function  $\mathcal{R}_{\text{ss}}(f)$  is much smaller than that of the Michelson channel  $\mathcal{R}_{\text{m}}(f)$  especially in the lower frequency range

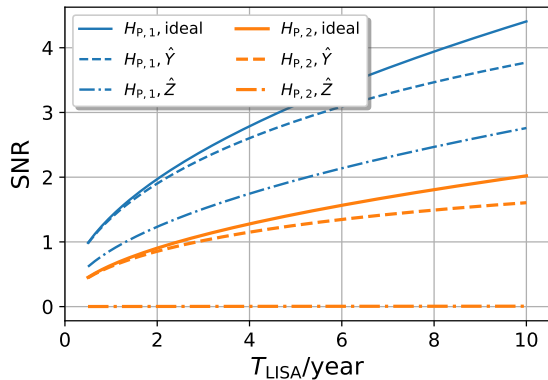


FIG. 4. SNRs of different estimators in the case of one LISA detector.

[41, 55–57]. In combination with the outputs of the two channels, it is natural to write the SGWB estimator as

$$\hat{X} = \int_{-\infty}^{\infty} df \int_{-\infty}^{\infty} df' \delta_T(f - f') \times [s_m^*(f) s_m(f') - W(f) s_{ss}^*(f) s_{ss}(f')] Q(f), \quad (24)$$

where  $W(f) = P_m(f)/P_{ss}(f)$ , with  $P_{ss}(f)$  and  $P_m(f)$  being the detector noise spectral density of two channels [40, 41, 58]. The mean value and variance are

$$\langle \hat{X} \rangle = T \int_0^{\infty} H(f) [\mathcal{R}_m(f) - W(f) \mathcal{R}_{ss}(f)] Q(f) df, \\ \sigma_X^2 \approx 2T \int_0^{\infty} [P_m^2(f) - W(f) |P_{m,ss}(f)|^2] |Q(f)|^2 df.$$

where  $P_{m,ss}(f)$  is cross power of noises in the two channels. In the similar way, we can write the estimators  $\hat{Y}$  and  $\hat{Z}$  as in the case of two LISA detectors. We show the SNRs of different estimators for the SGWB with two different fiducial spectral densities in Fig. 4. As in the two-detectors case, the foreground cleaning increases the LISA sensitivity by 30% – 50% for model  $H_{P,1}(f)$ , and it enables the detection for  $H_{P,2}(f)$ . Compared with the case of two detectors (Fig. 3), the SNRs of different estimators here turn out to be smaller by a factor  $2 \sim 4$ .

### Foreground cleaning by event-based subtraction

In the main text, we reconstructed the underlying distribution of BBH mergers from all the mergers recorded by the CE following the statistical approach of Eq. (2). Now we explore the foreground measurement of event-to-event approach following Eq. (1). Assume the LISA runs from  $-T/2$  to  $T/2$ , and the CE runs from  $-T/2$  to  $-T/2 + T_{CE}$ . For each BBH in the LISA band, we expect to detect its merger after some time  $t$  in the CE band,

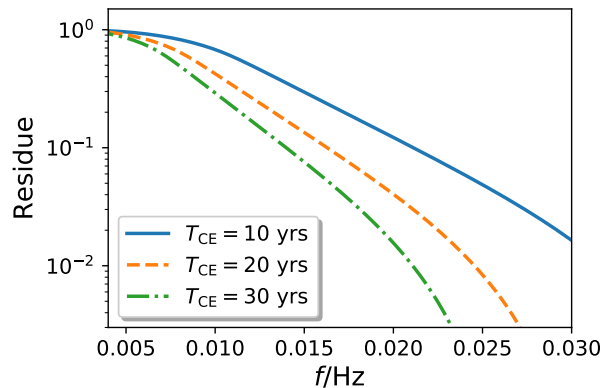


FIG. 5. The performance of foreground cleaning with event-based subtraction.

where  $t$  is determined by the GW frequency evolution equation [see e.g., Ref. 53]

$$\frac{dt}{df} = \frac{5}{96\pi^{8/3}} \frac{f^{-11/3}}{[GM_c(1+z)]^{5/3}}, \quad (25)$$

and we can add up the contribution to the LISA band foreground from BBHs which merger during the CE running phase,

$$\hat{H}_A(f)|_{CE} = \frac{1}{T} \sum_j (|h_+(f)|^2 + |h_\times(f)|^2)_j \Theta_T^j(f) df,$$

where  $j$  runs over all mergers detected by the CE. If the CE runs for a infinitely long time  $T_{CE} \rightarrow \infty$ ,  $\hat{H}_A(f)|_{CE} \rightarrow \hat{H}_A(f)$ . For a finite CE running time, only a fraction of BBHs in the LISA band will evolve into merger phase and the expectation value turns out to be

$$\langle \hat{H}_A(f) |_{CE} \rangle = \int_{z=z_{\min}(f, M_c)}^{z=\infty} \int_{M_{c, \min}}^{M_{c, \max}} \sum_A |h_A(f)|^2 \times \frac{R(z)}{1+z} dV_c(z) p(M_c) dM_c, \quad (26)$$

where  $z_{\min}(f, M_c)$  is determined by Eq. (25)

$$T_{CE} = \frac{15}{768\pi^{8/3}} \frac{f^{-8/3}}{[GM_c(1+z_{\min})]^{5/3}}, \quad (27)$$

where we have used the fact that the BBH merger frequency is well above the LISA band frequency  $f$ .

In Fig. 5, we show the residue fraction after the event-to-event cleaning  $1 - \langle \hat{H}_A(f) |_{CE} \rangle / \langle \hat{H}_A(f) \rangle$  given a finite running CE time ( $T_{CE} = 10, 20, 30$  years). It takes longer time for binaries of lower frequency to merge, therefore lower-frequency foreground cleaning is slower. With the CE running for 10 years, the astrophysical foreground can be cleaned to percent level for  $f \gtrsim 0.03$  Hz. Therefore the foreground cleaning of distribution-based approach is more efficient than that of event-based approach.